BMC Ophthalmology

RESEARCH

Open Access

Choroidal vascular changes in eyes with acute macular neuroretinopathy and paracentral acute middle maculopathy: new insights

Nicola Valsecchi[1,2*], Matteo Elifani[1,2], Chiara Veronese[2], Emilia Maggio[3], Antonio Moramarco[1,2], Mohammed Abdul Rasheed[4], Grazia Pertile[3], Kiran Kumar Vupparaboina[4], Jay Chhablani[4], Luigi Fontana[1,2] and Maurizio Mete[1,2]

Abstract

Purpose To assess choroidal vasculature changes in acute macular neuroretinopathy (AMN) and paracentral acute middle maculopathy (PAMM) during the acute and resolution phases.

Methods Retrospective, cross-sectional study. Twenty-eight eyes from 28 patients were analyzed: 8 with AMN and 20 with PAMM. Also, 30 healthy age-matched controls were included. Clinical records and spectral-domain optical coherence tomography (SD-OCT) scans from patients with AMN and PAMM were assessed. Choroidal assessment was performed using an automated algorithm, binarized into stromal choroidal areas (SCA) and luminal choroidal areas (LCA). Choroidal vascularity index (CVI) was calculated as the ratio of LCA to total choroidal area (TCA). Statistical analysis was performed using non-parametric tests.

Results The median age was 54 years (IQR = 32-68.5), and 60.7% were female. AMN eyes showed significantly increased subfoveal choroidal thickness (SFCT), TCA, SCA, and LCA compared to PAMM and controls ($p = 0.044$, $p = 0.007$, $p = 0.002$, $p = 0.014$ respectively). No differences in CVI were observed between the groups ($p = 0.535$). These findings remained consistent when comparing AMN with isolated PAMM and PAMM associated with retinal vascular diseases ($p < 0.05$). SFCT, TCA, SCA, and LCA significantly decreased in AMN eyes ($p = 0.045$, $p = 0.041$, $p = 0.040$, $p = 0.038$ respectively) after resolution, while no changes were observed in PAMM ($p > 0.05$). Also, resolved AMN exhibited higher SFCT, TCA, SCA and LCA compared to controls and resolved PAMM eyes ($p < 0.05$).

Conclusions Increased choroidal thickness is a characteristic feature of AMN, with reduction observed after resolution. On the other hand, no changes were observed in PAMM, suggesting distinct pathophysiological mechanisms between the two conditions.

Keywords Choroid, AMN, PAMM, Pathogenesis

*Correspondence:
Nicola Valsecchi
nicola.valsecchi2@studio.unibo.it
[1]Ophthalmology Unit, Dipartimento di Scienze Mediche e Chirurgiche, Alma Mater Studiorum University of Bologna, Bologna, Italy
[2]IRCCS Azienda Ospedaliero-Universitaria di Bologna, Via Pelagio Palagi 9, Bologna, Postal code, 40138 Bologna, Italy
[3]Department of Ophthalmology, IRCCS Sacro Cuore-Don Calabria Hospital, 3024 Negrar, Italy
[4]Department of Ophthalmology, School of Medicine, University of Pittsburgh, Pittsburgh, PA, USA

Introduction

Acute macular neuroretinopathy (AMN) is a rare macular condition first described by Bos and Deutman in 1975, with a prevalence ranging from 0.66 to 8.97 cases per 100.000 visits [1, 2]. Clinically, it is characterized by the acute onset of photopsia and paracentral scotoma, accompanied by reduction in visual acuity. It primarily affects young adults, with a higher prevalence among females and Caucasians [3]. Among the identified triggering factors, a history of viral symptoms or fever, and the use of oral contraceptives were the most frequently reported [4]. The advent of optical coherence tomography (OCT) has significantly improved the characterization of AMN [5]. In the acute phase, the condition is distinguished by hyperreflectivity of the outer plexiform layer, followed by thinning of the outer nuclear layer and disruption of the photoreceptor layer and retinal pigment epithelium (RPE).

On the other hand, paracentral acute middle maculopathy (PAMM) is an OCT finding associated with vaso-occlusive retinal conditions of both arterial and venous origin [6]. Initially classified as a variant of AMN, OCT imaging enabled its differentiation based on distinct features, such as the hyperreflectivity of the inner nuclear layer (INL), which subsequently results in thinning of the INL. This distinction has led to the classification of PAMM as a separate clinical entity from AMN [7]. Although AMN and PAMM are distinct conditions, they share overlapping characteristics, especially with regard to their presumed ischemic etiology. Furthermore, PAMM and AMN can coexist within the same eye, suggesting a common pathophysiologic mechanism [8].

Numerous studies utilizing OCT angiography (OCTA) have provided strong evidence that the deep capillary plexus (DCP) is the primary site of damage in PAMM, with associated reductions in vascular flow [9, 10]. Conversely, the precise localization of ischemic insult in AMN remains a subject of ongoing debate. Historically, capillary flow deficit at the level of the DCP was considered the primary pathogenic mechanism in AMN [11, 12]. However, over the past years, increasing attention has shifted toward alterations in the choriocapillaris (CC) [13, 14]. Recently, Hashimoto et al. reported a single case of bilateral AMN in a 15-year-old male, characterized by an increase in subfoveal choroidal thickness (SFCT) and alterations in choroidal circulation during the acute phase of the disease. These findings resolved over time, supporting the hypothesis of an involvement of the choroidal vasculature [15]. Also, von der Burchard et al. identified a perfusion deficit in the CC and choroidal layer in AMN, suggesting that choroidal hypoperfusion, rather than the previously believed hypoperfusion of the deep capillary plexus (DCP), is the primary mechanism underlying AMN. However, the study lacked longitudinal assessment of patients before and after resolution of the acute event, and they did not include OCT parameters such as choroidal thickness or the choroidal vascularity index (CVI).

Therefore, the present study aimed to assess the changes in the choroidal vasculature in AMN by quantifying the choroidal thickness and the CVI in the acute phase and after resolution of the disease. To improve measurement accuracy, we used a previously validated artificial intelligence (AI)-based software [16]. In addition, we sought to compare these findings with a cohort of PAMM cases to further refine the distinction between these two clinical entities.

Materials and methods

Study population

This retrospective, observational, multicentric study included patients diagnosed with PAMM and AMN lesions, based on clinical examination and OCT findings. Patients were recruited from the Unit of Ophthalmology, IRCCS University of Bologna (Bologna, Italy) and from the Department of Ophthalmology, IRCCS Sacro Cuore-Don Calabria Hospital (Negrar, Italy). Institutional review board approval was obtained from the respective referral centers for the retrospective chart review. The study adhered to the principles of the Declaration of Helsinki, and all participants provided written informed consent. Diagnostic criteria for acute AMN included the presence of an acute paracentral scotoma corresponding to hyperreflective lesions in the outer retina, accompanied by disruption of the ellipsoid zone (EZ). For PAMM, diagnostic criteria involved a recent history of acute paracentral scotomas, with or without deep intraretinal whitening on fundus examination, hyporeflective wedge-shaped lesions on near infrared reflectance (NIR) imaging, and corresponding hyperreflective lesions in the INL on OCT, as previously described [8]. Furthermore, patients were divided based on the presence of PAMM into those with concomitant retinal vascular conditions and those with isolated PAMM. Resolution of the acute phase was considered at least 3 months after the event, with the disappearance of acute signs on OCT scans. Exclusion criteria were significant media opacities, other macular conditions (e.g., intermediate or late-stage age-related macular degeneration or diabetic macular edema), poor-quality imaging, any prior ocular surgeries (except cataract surgery), and high myopia or hyperopia. A cohort of healthy age-matched controls was also included, following the same exclusion criteria.

Ophthalmological assessment

At baseline and follow-up visits after disease resolution, a comprehensive ophthalmological examination was performed, which included measurement of BCVA,

slit-lamp biomicroscopy, intraocular pressure (IOP) assessment, dilated fundus examination using a 90D indirect lens, and spectral-domain (SD)-OCT imaging (Spectralis HRA-OCT; Heidelberg Engineering GmbH, Heidelberg, Germany). BCVA was assessed using a Snellen chart and converted to the logarithm of the minimum angle of resolution (logMAR) for statistical analysis.

OCT image acquisition

All subjects underwent the same SD-OCT protocol using the Heidelberg Spectralis system in high-resolution (HR) mode (Heidelberg Engineering, Germany), which included a dense 20° × 15° raster scan with 19 B-scans spaced 250 µm apart, along with two vertical and horizontal single scans centered on the fovea (with automatic real-time values of at least 14 or higher). Registered and tracked OCT scans from the first and last available visits were obtained for each patient. The subfoveal choroidal thickness (SFCT) was manually measured as the vertical distance between the hyperreflective line of the Bruch membrane and the inner scleral surface using the caliper tool in the image analysis software. Measurements were performed by two independent observers (E.M, M.E.), with discrepancies resolved by a third observer (M.M.).

Choroidal vascularity index analysis

To assess the CVI, SD-OCT (Heidelberg Engineering, Heidelberg, Germany) images were used. OCT scans were performed between 9:00 AM and 12:00 PM to minimize diurnal variation effects on choroidal parameters. Registered and tracked OCT scans were used to assess the choroidal vasculature at baseline and after resolution. CVI was measured using an AI-based automated algorithm that included shadow compensation, denoising, localization of the inner and outer choroidal boundaries, and segmentation of the choroidal region from the rest of the scan [16]. Binarization of the choroid generated bright regions labeled as stromal choroidal areas (SCA) and dark regions labeled as luminal choroidal areas (LCA). CVI was calculated as the ratio of the luminal choroidal area to the total choroidal area (TCA). See Fig. 1.

Statistical analysis

Given the small sample sizes and the non-normal distribution of the data, non-parametric tests were employed. As variables were not normally distributed, they were reported as medians with interquartile ranges (IQR). Fisher's exact test was used to assess associations between categorical variables. The Kruskal-Wallis test was applied to compare choroidal biomarkers among the AMN, PAMM and healthy eyes, and among AMN, isolated PAMM, and PAMM associated with retinal vascular diseases. Pairwise comparisons using the Dunn-Bonferroni approach were performed for significant variables. The Wilcoxon signed-rank test was used to compare choroidal biomarkers at baseline and after disease resolution. Mann-Whitney U tests were performed to compare AMN with healthy controls, PAMM with healthy controls, and PAMM with AMN eyes. P-values < 0.05 were considered statistically significant. All statistical analyses were conducted using IBM SPSS Statistics version 26.

Results

Demographic data

A total of 28 eyes of 28 patients were included in the analysis, 8 eyes with AMN, and 20 eyes with PAMM. Also, 30 eyes of 30 healthy age-matched controls were included in the analysis. Demographics are shown in Table 1.

No differences in terms of age and sex were observed between the three groups. Median visual acuity was 0.1 LogMar (IQR = 0.05–0.3) in the AMN group and 0.5 LogMar (IQR = 0.2–0.7) in the PAMM group. In the AMN group, one patient underwent a previous bone marrow transplant for acute myeloid leukemia, and three patients had a previous flu-like illness. The remaining five patients did not present concomitant comorbidities at the time of the acute event. In the PAMM group, 5 patients had a concomitant branch retinal artery occlusion (BRAO), 2 patients had concomitant central retinal artery occlusion (CRAO), 3 patients had central retinal vein occlusion (CRVO), and 1 patient branch retinal vein occlusion (BRVO). The remaining 9 patients presented isolated PAMM. Among these patients, 6 did not have any concomitant comorbidities, 2 patients had a history

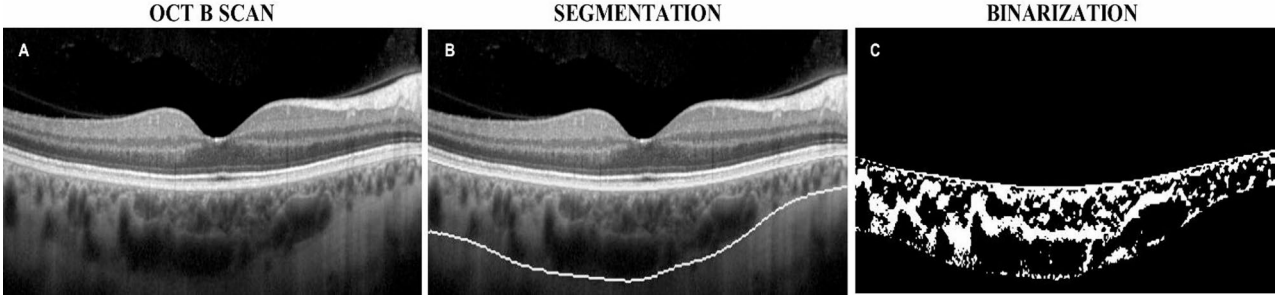

Fig. 1 Choroidal vascularity index analysis. (**A**) OCT foveal scan is shown; (**B**) Choroidal area segmentation; (**C**) Choroidal area binarization

Table 1 Demographic data and choroidal biomarkers in acute macular neuroretinopathy (AMN), paracentral acute middle maculopathy (PAMM), and healthy age-matched controls

	Controls ($n=30$)	PAMM ($n=20$)	AMN ($n=8$)	*P* value
Age, median ± IQR	51 (28–65.5)	54 (44-63.5)	48 (31–52.5)	0.101
Sex female, number (%)	14 (46.67%)	11 (55%)	6 (75%)	0.314
SFCT, μm median (IQR)	280.5 (231-352.25)	283 (218-335.5)	512 (321.2–565.1)	**0.044**
TCA, mm2 median (IQR)	1.55 (1.28–1.94)	1.74 (1.12–1.85)	2.72 (2.32–3.86)	**0.007**
SCA, mm2 median (IQR)	0.58 (0.48–0.73)	0.68 (0.54–0.71)	1.12 (0.98–1.61)	**0.002**
LCA, mm2 median (IQR)	0.99 (0.76–1.16)	0.96 (0.72–1.13)	1.48 (1.12–2.26)	**0.014**
CVI, % median (IQR)	62 (59.75-65)	62 (57–64)	62 (56.5–63.5)	0.535

SFCT=subfoveal choroidal thickness, TCA=total choroidal area, SCA=stromal choroidal area, LCA=luminal choroidal area, CVI=choroidal vascularity index, IQR=interquartile range

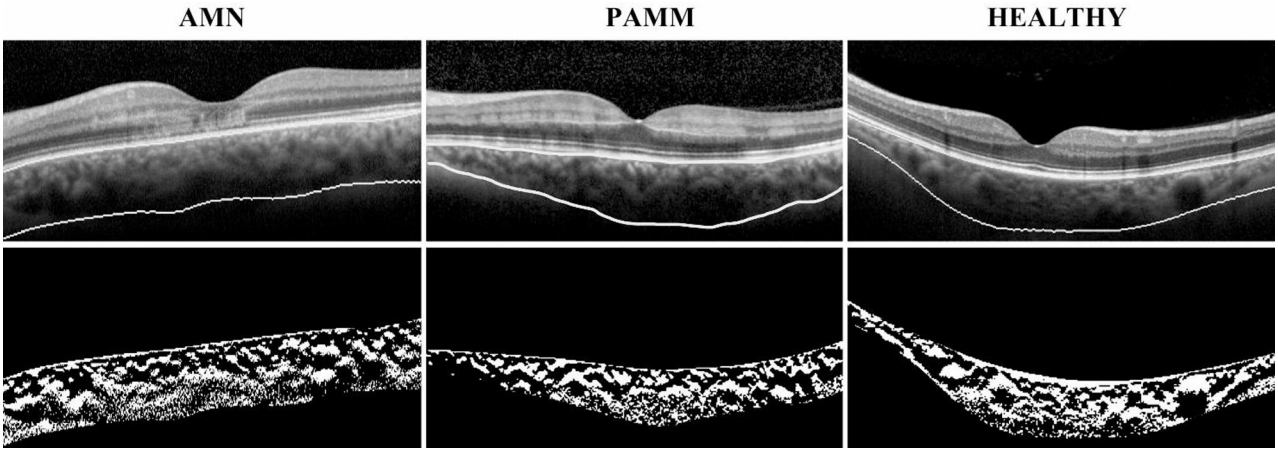

Fig. 2 Choroidal vascularity index analysis in acute macular neuroretinopathy (AMN), paracentral acute middle maculopathy (PAMM), and healthy controls. Note the increased choroidal thickness in a 34 years old female with AMN compared to a 32 years old female with PAMM, and a 30 years old healthy female

of ischemic stroke, and one patient had a homolateral carotid artery stenosis.

Choroidal parameters in AMN, PAMM, and healthy age-matched controls

Eyes with AMN presented an increased SFCT, TCA, SCA, and LCA compared to PAMM and controls. After Dunn-Bonferroni correction, TCA, SCA, and LCA remained statistically significant when comparing AMN and PAMM ($p=0.013$, $p=0.002$, $p=0.016$ respectively), and when comparing AMN and age-matched controls ($p=0.008$, $p=0.011$, $p=0.018$ respectively). On the other hand, SFCT was significantly increased in AMN eyes compared to PAMM ($p=0.048$), and it was close to significance when comparing AMN to healthy age-matched controls ($p=0.060$). No significant differences in CVI were observed among the three groups. See Table 1; Fig. 2.

Choroidal parameters in AMN, PAMM associated with concomitant retinal vascular diseases, isolated PAMM

Eyes with AMN presented an increased SFCT, TCA, SCA, and LCA compared to isolated PAMM and PAMM associated with concomitant retinal vascular diseases. After Dunn-Bonferroni correction, SFCT, TCA, SCA, LCA remained statistically significant when comparing AMN and PAMM with concomitant retinal vascular diseases ($p=0.042$, $p=0.015$, $p=0.004$, $p=0.014$ respectively), and when comparing AMN and isolated PAMM ($p=0.048$, $p=0.014$, $p=0.018$, $p=0.026$ respectively). No significant differences in CVI were observed among the three groups. See Table 2.

Choroidal parameters after resolution

After a median follow-up of 33.82 weeks (range 11–48 weeks), BCVA improved to 0 (IQR = 0-0.07) LogMar in the AMN group and to 0.3 (IQR = 0.1–0.6) LogMar in the PAMM group. SFCT, TCA, SCA, and LCA significantly decreased in AMN eyes. Choroidal thickness reduction after resolution of the acute event was observed in 100% of our cases in the AMN group. No significant differences were observed in CVI measurements. On the other hand, PAMM eyes presented a reduction in SFCT, TCA, SCA, LCA, and CVI, even though the results were not statistically significant. See Table 3. Representative cases are shown in Figs. 3 and 4.

Table 2 Demographic data and choroidal biomarkers in acute macular neuroretinopathy (AMN), paracentral acute middle maculopathy (PAMM) with concomitant retinal vascular diseases, and isolated PAMM cases

	PAMM with concomitant retinal vascular diseases ($n=11$)	Isolated PAMM ($n=9$)	AMN ($n=8$)	*P* value
Age, median ± IQR	**56 (48–67)**	**52 (44–58)**	**48 (31–52.5)**	**0.125**
Sex female, number (%)	6 (54.5%)	5 (55.5%)	6 (75%)	0.287
SFCT, μm median (IQR)	278 (205–330)	288 (225–341)	512 (321.2–565.1)	**0.043**
TCA, mm2 median (IQR)	1.70 (1.01–1.78)	1.77 (1.23–1.93)	2.72 (2.32–3.86)	**0.009**
SCA, mm2 median (IQR)	0.66 (0.52–0.68)	0.69 (0.61–0.75)	1.12 (0.98–1.61)	**0.004**
LCA, mm2 median (IQR)	0.94 (0.72–1.07)	0.97 (0.76–1.18)	1.48 (1.12–2.26)	**0.016**
CVI, % median (IQR)	62 (55–65)	62 (56.5–64.5)	62 (56.5–63.5)	0.671

SFCT=subfoveal choroidal thickness, TCA=total choroidal area, SCA=stromal choroidal area, LCA=luminal choroidal area, CVI=choroidal vascularity index, IQR=interquartile range

Table 3 Choroidal parameters before and after resolution in acute macular neuroretinopathy (AMN), isolated paracentral acute middle maculopathy (PAMM), and PAMM with concomitant retinal vascular diseases

Group	Baseline	Resolution	*P* value
AMN			
SFCT, μm median (IQR)	512 (321.2–565.1)	435 (261.5-486.5)	**0.045**
TCA, mm2 median (IQR)	2.72 (2.32–3.86)	1.92 (1.76–2.50)	**0.041**
SCA, mm2 median (IQR)	1.12 (0.98–1.61)	0.80 (0.65–0.99)	**0.040**
LCA, mm2 median (IQR)	1.48 (1.12–2.26)	1.18 (1.08–1.52)	**0.038**
CVI, % median (IQR)	62 (56.5–63.5)	61 (58.5–64.5)	0.465
PAMM with concomitant retinal vascular diseases			
SFCT, μm median (IQR)	278 (205–330)	262 (216–347)	0.231
TCA, mm2 median (IQR)	1.70 (1.01–1.78)	1.53 (1.18–2.15)	0.421
SCA, mm2 median (IQR)	0.66 (0.52–0.68)	0.53 (0.42–0.88)	0.294
LCA, mm2 median (IQR)	0.94 (0.72–1.07)	0.84 (0.70–1.23)	0.551
CVI, % median (IQR)	62 (55–65)	62 (0.59–0.64)	0.824
Isolated PAMM			
SFCT, μm median (IQR)	288 (225–341)	270 (242–358)	0.345
TCA, mm2 median (IQR)	1.77 (1.23–1.93)	1.60 (1.28–2.4)	0.528
SCA, mm2 median (IQR)	0.69 (0.61–0.75)	0.55 (0.48–0.91)	0.401
LCA, mm2 median (IQR)	0.97 (0.76–1.18)	0.83 (0.62–1.17)	0.231
CVI, % median (IQR)	62 (56.5–64.5)	62 (0.58–0.63)	0.897

IQR=interquartile range, SFCT=subfoveal choroidal thickness, TCA=total choroidal area, SCA=stromal choroidal area, LCA=luminal choroidal area, CVI=choroidal vascularity index

When comparing eyes with resolved AMN to healthy age-matched controls, we observed an increase in SFCT, TCA, SCA, and LCA, whereas no changes were observed for CVI. Also, AMN eyes showed a significant increase in SFCT, TCA, SCA and LCA compared to PAMM eyes. Conversely, PAMM eyes presented lower values of SFCT, TCA, SCA, LCA, and CVI compared to healthy controls, but the results were not statistically significant. See Table 4.

Discussion

In the present study, eyes with AMN presented an increased choroidal thickness compared to healthy eyes and PAMM. These findings remained consistent when comparing AMN with isolated PAMM and PAMM associated with retinal vascular diseases. Also, AMN eyes showed a significant reduction of the choroidal thickness after resolution. In contrast, we did not observe any significant differences in choroidal parameters in PAMM eyes before and after resolution. Furthermore, choroidal thickness was consistently increased in AMN eyes compared to healthy and PAMM eyes even after resolution.

Several studies suggested that PAMM is the result of INL infarction due to vascular impairment occurring at the DCP [17]. In contrast, controversy still exists regarding the pathogenesis of AMN. Pecen et al. and Nemiroff et al. demonstrated capillary flow impairment at the level of the DCP in AMN [18, 19]. Dansingani and Freund suggested that the perfusion deficit in AMN at the level of the DCP may not be severe enough to cause the typical alterations seen in PAMM. Instead, the characteristic changes at the photoreceptor level are likely a consequence of an ischemic event at the level of the CC [20]. Thanos and associates supported the theory that AMN may result from a vascular insult in the CC [21]. Furthermore, Lee et al. presented a case series of seven AMN patients, where OCTA imaging revealed flow deficits at the CC level during the acute phase of the disease. These perfusion abnormalities were correlated with the characteristic lesions observed on infrared imaging and, at the histological level, with the honeycomb-like microstructure of the choriocapillaris [22]. Recently, Duan et al. observed a topographic correlation between the neuroretinal lesions characteristic of AMN and the watershed zones at the choroidal level or areas of delayed choroidal perfusion, suggesting that increased vulnerability to hypoperfusion events may result from the presence of a double watershed zone, one between the DCP and the CC and the other at the choroidal watershed zones themselves [23]. Again, Hashimoto et al. described the case of a patient in which the choroid at the macula thickened at the onset of AMN and became thin with the regression of disease, suggesting that eyes with AMN may have blood flow impairments at the level of not only the CC but also the choroidal deeper layers [15]. Consistent with these studies, our findings indicate that choroidal thickness

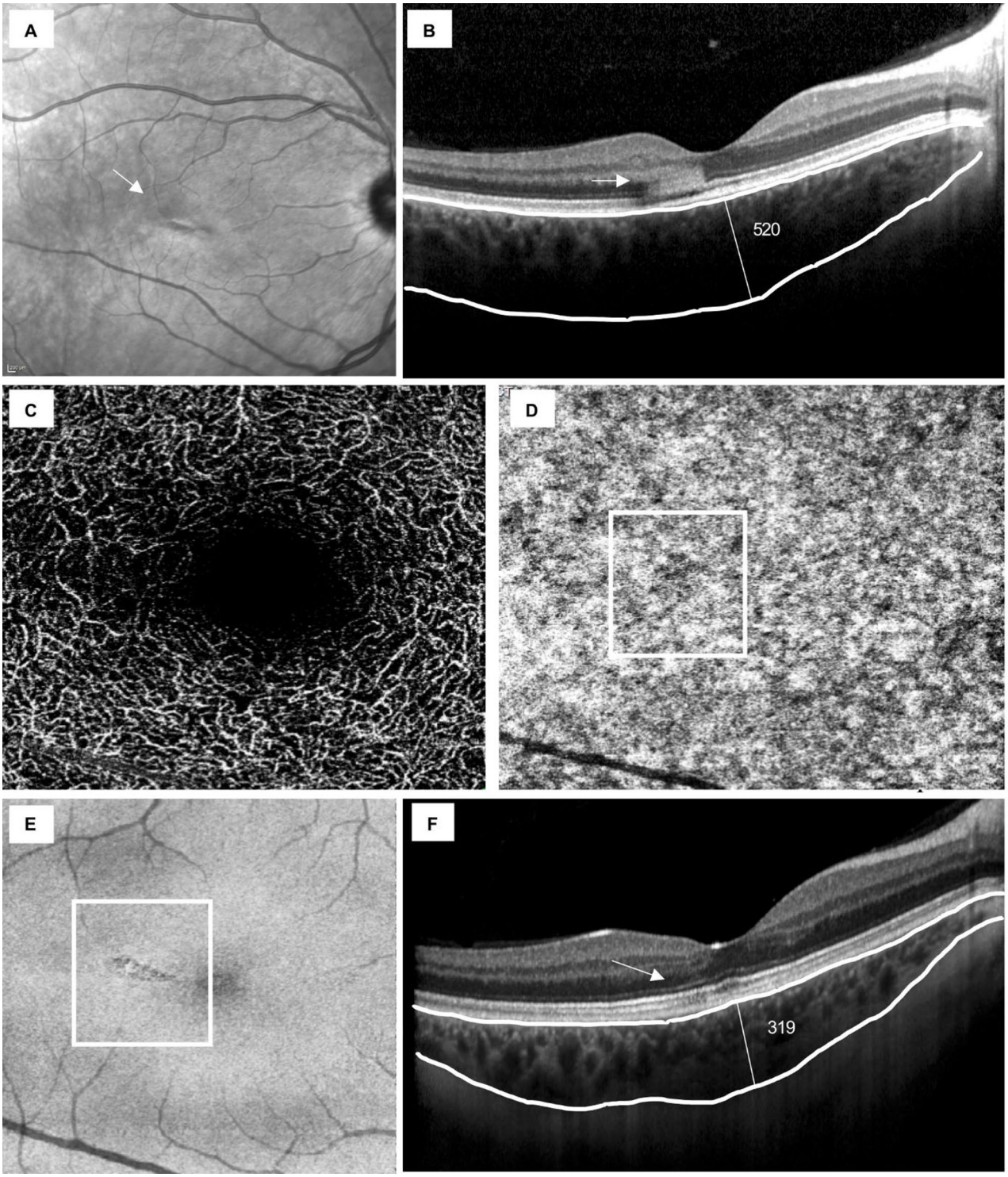

Fig. 3 Representative case of acute macular neuroretinopathy (AMN) at presentation (**A**-**B**) and after resolution (**C**-**F**). (**A**) Near-infrared (NIR) image at the presentation of the right eye in a 32 years old female: a wedge-shaped macular lesion (white arrow) with its apex directed toward the fovea is shown. (**B**) Spectral-domain optical coherence tomography (SD-OCT) horizontal foveal scan shows a hyper-reflective band at the level of the outer plexiform layer (OPL) (white arrow). The subfoveal choroidal thickness (SFCT) is 520 μm. (**C**) After 10 months from the acute event, a 3 mm x 3 mm macular cube optical coherence tomography angiography (OCTA) does not show alterations at the level of deep capillary plexus (DCP). (**D**) On the other hand, attenuation of the choriocapillaris (white box) is observed, which corresponds to the enface OCT scan (**E**) at the level of the IS/OS-ellipsoid layer, revealing a wedge-shaped lesion (white box). (**F**) SD-OCT horizontal foveal scan shows disruption of the ellipsoid zone and the interdigitation zone (white arrow). SFCT is 319 μm

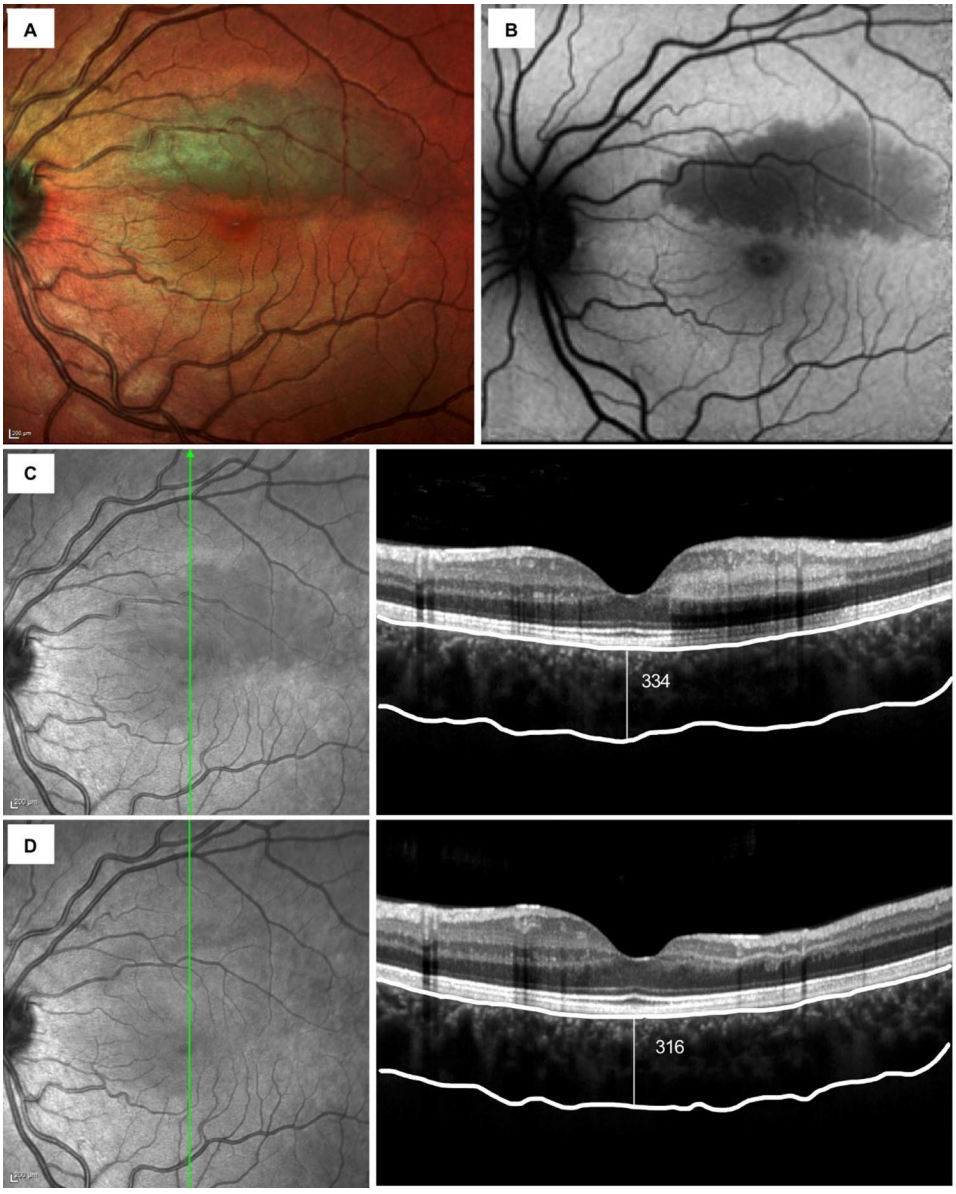

Fig. 4 Representative case of paracentral acute middle maculopathy (PAMM) at presentation (**A**-**C**) and after resolution (**D**): Multicolor (**A**) and fundus autofluorescence (**B**) display the PAMM lesion in a 34 years old female. (**A**) Shows a whitish lesion, and (**B**) shows a hypoautofluorescent lesion. (**C**) Near-infrared (NIR) and spectral-domain optical coherence tomography (SD-OCT) vertical foveal scan at presentation are shown. A placoid, hyperreflective band involving the inner nuclear layer with associated shadowing of outer layers is displayed. Subfoveal choroidal thickness (SFCT) is 334 μm (**D**). After 7 months from the acute event, thinning of the inner retinal layer is observed in the area of PAMM. SFCT is 316 μm

increases in AMN and decreases following the resolution of the acute event, whereas eyes with PAMM did not show significant changes in the choroidal vasculature. These results support the hypothesis that choroidal involvement occurs in AMN but not in PAMM, suggesting distinct pathophysiological mechanisms between the two conditions.

As previously described, ocular pathologies characterized by an inflammatory process at the choroidal level show choroidal thickening during the acute phases, which then, in the remission phase, results in a reduction of the choroidal thickness [24]. Mrejen et al. reported an increase in choroidal thickness in acute posterior multifocal placoid pigment epitheliopathy (APMPPE), which subsequently decreased following resolution of the disease, suggesting that a transient ischemic choroiditis may contribute to secondary damage of the RPE [25]. Pellegrini et al. observed an increase in choroidal thickness, TCA, and CVI in eyes with multiple evanescent white dots syndrome (MEWDS), with these choroidal alterations being transient, suggesting that the observed increase in the vascular component is likely

Table 4 Comparison of choroidal parameters in resolved acute macular neuroretinopathy (AMN), resolved paracentral acute middle maculopathy (PAMM), and healthy controls

	Controls (*n* = 30)	**Resolved AMN (*n* = 8)**	***P* value**
SFCT, μm median (IQR)	**280.5 (231-352.25)**	**435 (261.5-486.5)**	**0.031**
TCA, mm2 median (IQR)	1.55 (1.28–1.94)	1.92 (1.76–2.50)	**0.036**
SCA, mm2 median (IQR)	0.58 (0.48–0.73)	0.80 (0.65–0.99)	**0.023**
LCA, mm2 median (IQR)	0.99 (0.76–1.16)	1.18 (1.08–1.52)	**0.045**
CVI, % median (IQR)	62 (59.75-65)	61 (58.5–64.5)	0.562
	Controls (*n* = 30)	**Resolved PAMM)** (*n* = 20	**P value**
SFCT, μm median (IQR)	280.5 (231-352.25)	262 (216–347)	0.567
TCA, mm2 median (IQR)	1.55 (1.28–1.94)	1.53 (1.18–2.15)	0.686
SCA, mm2 median (IQR)	0.58 (0.48–0.73)	0.53 (0.42–0.88)	0.821
LCA, mm2 median (IQR)	0.99 (0.76–1.16)	0.84 (0.70–1.23)	0.743
CVI, % median (IQR)	62 (59.75-65)	62 (0.59–0.64)	0.673
	Resolved AMN (*n* = 8)	**Resolved PAMM** (*n* = 20)	**P value**
SFCT, μm median (IQR)	435 (261.5-486.5)	262 (216–347)	**0.043**
TCA, mm2 median (IQR)	1.92 (1.76–2.50)	1.53 (1.18–2.15)	**0.032**
SCA, mm2 median (IQR)	0.80 (0.65–0.99)	0.53 (0.42–0.88)	**0.033**
LCA, mm2 median (IQR)	1.18 (1.08–1.52)	0.84 (0.70–1.23)	**0.030**
CVI, % median (IQR)	61 (58.5–64.5)	62 (0.59–0.64)	0.468

SFCT=subfoveal choroidal thickness, TCA=total choroidal area, SCA=stromal choroidal area, LCA=luminal choroidal area, CVI=choroidal vascularity index, IQR=interquartile range

due to vascular stasis associated with the inflammatory process [26]. In our study, we observed an increase in SFCT, TCA, SCA, and LCA in AMN, supporting the hypothesis that an active inflammatory process might occur in the choroid during the acute phase. However, the CVI value remained unchanged, which may be due to a concurrent increase in both the vascular component, resulting from vascular stasis, and the stromal component, leading to no significant alteration in the CVI. This finding suggests that AMN may involve pathophysiological mechanisms distinct from those observed in classic inflammatory chorioretinal disorders. It is noteworthy that in resolved cases of AMN, choroidal biomarkers remained significantly elevated compared to the control group, supporting the hypothesis of lasting alterations in both the choroidal vascular and stromal components following the acute inflammatory process in AMN. Overall, our results indicate that the choroid may play a role in the acute phase of AMN. However, this interpretation remains speculative, and further studies with larger patient cohorts are necessary to clarify the underlying mechanisms.

The main limitation of this study is the small number of eyes included in the AMN group, which reduces the statistical power and increases susceptibility to outlier effects, limiting the generalizability of the findings. Nevertheless, the cohort is carefully characterized, which represents a strength given the rarity of AMN. Larger studies will be needed in the future to more robustly compare choroidal changes between AMN, PAMM, and healthy controls. Additionally, the relatively short follow-up period may not capture long-term changes; thus, extended follow-up is necessary to assess the lasting effects on choroidal vasculature in AMN and PAMM. Also, CVI and choroidal thickness can be influenced by several factors, including diurnal variations, age, and sex, and refractive errors [27]. To minimize potential confounding factors, OCT examinations were conducted at a consistent time of day to account for diurnal variations, patients were matched for age and sex, and subjects with high refractive errors were excluded. Another limitation is the absence of OCTA images for all study participants, which prevented the analysis of the choriocapillaris and the DCP. Future research should incorporate multimodal imaging to correlate the CVI measures with OCTA parameters for a more comprehensive analysis.

Conclusions

Our study demonstrated an increase in choroidal thickness in AMN, which subsequently decreased following resolution. Also, eyes with AMN presented an increased choroidal thickness compared to healthy controls even after resolution, suggesting that choroidal alterations persist after recovery. In contrast, no significant changes in choroidal parameters were observed in eyes with PAMM. These findings lend support to the hypothesis that AMN may primarily result from choroidal alterations, suggesting distinct pathophysiological mechanisms compared to PAMM. However, this hypothesis remains speculative, and further investigations are required to determine whether ischemic processes alone are responsible or if inflammatory mechanisms also contribute to the development of the disease.

Acknowledgements
None.

Author contributions
Valsecchi N., Elifani M., Mete M., Maggio E., and Veronese C. conceived and designed the study. Valsecchi N., Elifani M., Maggio E., and Vupparaboina K. K. Acquired, analyzed, and interpreted the data. Valsecchi N. performed statistical analysis. Valsecchi N. and Elifani M. drafted the article. Mete M., Veronese C., Maggio E., Moramarco A., Fontana L., Chhablani J., and Pertile G. revised it for intellectual content. The final version of the manuscript was approved by all the authors.

Funding
None.

Data availability
The datasets used and/or analysed during the current study are available from the corresponding author on reasonable request.

Declarations

Ethics approval and consent to participate
The study adhered to the principles of the Declaration of Helsinki, and all participants provided written informed consent and agreed to participate in the study. This study was approved by the Ethics Committee of Bologna, Italy (Cod CE: 53/2025/Oss/AOUBo).

Consent for publication
All participants have given written permission to publish personal data.

Competing interests
The authors declare no competing interests.

Received: 27 July 2025 / Accepted: 6 February 2026
Published online: 11 February 2026

References

1. Bos PJM, Deutman AF. Acute macular neuroretinopathy. Am J Ophthalmol. 1975;80(4):573–84. https://doi.org/10.1016/0002-9394(75)90387-6.
2. Azar G, Bonnin S, Vasseur V, et al. Did the COVID-19 pandemic increase the incidence of acute macular neuroretinopathy? J Clin Med. 2021;10(21):5038. https://doi.org/10.3390/jcm10215038.
3. Miller MH, Spalton DJ, Fitzke FW, Bird AC. Acute macular neuroretinopathy. Ophthalmology. 1989;96(2):265–9. https://doi.org/10.1016/s0161-6420(89)32906-x.
4. Bhavsar KV, Lin S, Rahimy E, et al. Acute macular neuroretinopathy: a comprehensive review of the literature. Surv Ophthalmol. 2016;61(5):538–65. https://doi.org/10.1016/j.survophthal.2016.03.003.
5. Fawzi AA, Pappuru RR, Sarraf D, et al. Acute macular neuroretinopathy: long-term insights revealed by multimodal imaging. Retina Phila Pa. 2012;32(8):1500–13. https://doi.org/10.1097/IAE.0b013e318263d0c3.
6. Moura-Coelho N, Gaspar T, Ferreira JT, Dutra-Medeiros M, Cunha JP. Paracentral acute middle maculopathy-review of the literature. Graefes Arch Clin Exp Ophthalmol Albrecht Von Graefes Arch Klin Exp Ophthalmol. 2020;258(12):2583–96. https://doi.org/10.1007/s00417-020-04826-1.
7. Sarraf D, Rahimy E, Fawzi AA, et al. Paracentral acute middle maculopathy: A new variant of acute macular neuroretinopathy associated with retinal capillary ischemia. JAMA Ophthalmol. 2013;131(10):1275. https://doi.org/10.1001/jamaophthalmol.2013.4056.
8. Iovino C, Au A, Ramtohul P, et al. Coincident PAMM and AMN and insights into a common pathophysiology. Am J Ophthalmol. 2022;236:136–46. https://doi.org/10.1016/j.ajo.2021.07.004.
9. Shah A, Rishi P, Chendilnathan C, Kumari S. OCT angiography features of paracentral acute middle maculopathy. Indian J Ophthalmol. 2019;67(3):417–9. https://doi.org/10.4103/ijo.IJO_1249_18.
10. Casalino G, Williams M, McAvoy C, Bandello F, Chakravarthy U. Optical coherence tomography angiography in paracentral acute middle maculopathy secondary to central retinal vein occlusion. Eye. 2016;30(6):888–93. https://doi.org/10.1038/eye.2016.57.
11. Rahimy E, Sarraf D. Paracentral acute middle maculopathy spectral-domain optical coherence tomography feature of deep capillary ischemia. Curr Opin Ophthalmol. 2014;25(3):207–12. https://doi.org/10.1097/ICU.0000000000000045.
12. Rahimy E, Kuehlewein L, Sadda SR, Sarraf D. Paracentral acute middle maculopathy: what we knew then and what we know now. Retina Phila Pa. 2015;35(10):1921–30. https://doi.org/10.1097/IAE.0000000000000785.
13. Thanos A, Faia LJ, Yonekawa Y, Randhawa S. Optical coherence tomographic angiography in acute macular neuroretinopathy. JAMA Ophthalmol. 2016;134(11):1310–4. https://doi.org/10.1001/jamaophthalmol.2016.3513.
14. Lee SY, Cheng JL, Gehrs KM, et al. Choroidal features of acute macular neuroretinopathy via optical coherence tomography angiography and correlation with serial multimodal imaging. JAMA Ophthalmol. 2017;135(11):1177–83. https://doi.org/10.1001/jamaophthalmol.2017.3790.
15. Hashimoto Y, Saito W, Saito M, Hasegawa Y, Ishida S. Increased thickness and decreased blood flow velocity of the choroid in a patient with acute macular neuroretinopathy. BMC Ophthalmol. 2019;19(1):109. https://doi.org/10.1186/s12886-019-1123-0.
16. Agrawal R, Wei X, Goud A, Vupparaboina KK, Jana S, Chhablani J. Influence of scanning area on choroidal vascularity index measurement using optical coherence tomography. Acta Ophthalmol (Copenh). 2017;95(8):e770–5. https://doi.org/10.1111/aos.13442.
17. Fumi D, Ruggeri F, Fasciolo D, Antonello E, Burtini G, Abdolrahimzadeh S. Paracentral acute middle maculopathy (PAMM) in ocular vascular Diseases—What we know and future perspectives. Vision. 2025;9(1):19. https://doi.org/10.3390/vision9010019.
18. Pecen PE, Smith AG, Ehlers JP. Optical coherence tomography angiography of acute macular neuroretinopathy and paracentral acute middle maculopathy. JAMA Ophthalmol. 2015;133(12):1478. https://doi.org/10.1001/jamaophthalmol.2015.4100.
19. Nemiroff J, Sarraf D, Davila JP, Rodger D, Optical coherence tomography, angiography of acute macular neuroretinopathy reveals deep capillary ischemia. Retin Cases Brief Rep. 2018;12(1):S12–5. https://doi.org/10.1097/ICB.0000000000000706.
20. Dansingani KK, Freund KB. Paracentral acute middle maculopathy and acute macular neuroretinopathy: related and distinct entities. Am J Ophthalmol. 2015;160(1):1–e32. https://doi.org/10.1016/j.ajo.2015.05.001.
21. Thanos A, Faia LJ, Yonekawa Y, Randhawa S. Optical coherence tomographic angiography in acute macular neuroretinopathy. JAMA Ophthalmol. 2016;134(11):1310. https://doi.org/10.1001/jamaophthalmol.2016.3513.
22. Lee SY, Cheng JL, Gehrs KM, et al. Choroidal features of acute macular neuroretinopathy via optical coherence tomography angiography and correlation with serial multimodal imaging. JAMA Ophthalmol. 2017;135(11):1177. https://doi.org/10.1001/jamaophthalmol.2017.3790.
23. Duan J, An J, Li M, et al. Topographical relationship between acute macular neuroretinopathy and choroidal watershed zone or patchy choroidal filling. Front Med. 2022;9:762609. https://doi.org/10.3389/fmed.2022.762609.
24. Steiner M, Esteban-Ortega M, del Muñoz-Fernández M. Choroidal and retinal thickness in systemic autoimmune and inflammatory diseases: A review. Surv Ophthalmol. 2019;64(6):757–69. https://doi.org/10.1016/j.survophthal.2019.04.007.
25. Mrejen S, Sarraf D, Chexal S, Wald K, Freund KB. Choroidal involvement in acute posterior multifocal placoid pigment epitheliopathy. Ophthalmic Surg Lasers Imaging Retina. 2016;47(1):20–6. https://doi.org/10.3928/23258160-20151214-03.
26. Pellegrini M, Veronese C, Bernabei F, et al. Choroidal vascular changes in multiple evanescent white Dot syndrome. Ocul Immunol Inflamm. 2021;29(2):340–5. https://doi.org/10.1080/09273948.2019.1678650.
27. Sadeghi E, Valsecchi N, Rahmanipour E, et al. Choroidal biomarkers in age-related macular degeneration. Surv Ophthalmol. Published Online October 18, 2024:S0039-6257(24)00131-0. https://doi.org/10.1016/j.survophthal.2024.10.004.

Publisher's note